Journal of Medicinal Chemistry

Article

pubs.acs.org/jmc

Tricyclic Sulfonamides Incorporating Benzothiopyrano[4,3-*c*]pyrazole and Pyridothiopyrano[4,3-*c*]pyrazole Effectively Inhibit α- and β-Carbonic Anhydrase: X-ray Crystallography and Solution Investigations on 15 Isoforms

Anna M. Marini,*[,†] Alfonso Maresca,[‡] Mayank Aggarwal,[§] Elisabetta Orlandini,[†] Susanna Nencetti,[†] Federico Da Settimo,[†] Silvia Salerno,[†] Francesca Simorini,[†] Concettina La Motta,[†] Sabrina Taliani,[†] Elisa Nuti,[†] Andrea Scozzafava,[‡] Robert McKenna,[§] Armando Rossello,[†] and Claudiu T. Supuran*[,‡]

[†]Dipartimento di Scienze Farmaceutiche, Università di Pisa, Via Bonanno 6, 56126 Pisa, Italy

[‡]Università degli Studi di Firenze, Polo Scientifico, Laboratorio di Chimica Bioinorganica, Rm. 188, Via della Lastruccia 3, 50019 Sesto Fiorentino (Florence), Italy

[§]Department of Biochemistry and Molecular Biology, College of Medicine, University of Florida, Box 100245, Gainesville, Florida 32610, United States

Supporting Information

ABSTRACT: Carbonic anhydrases (CAs, EC 4.2.1.1) are ubiquitous isozymes involved in crucial physiological and pathological events, representing the targets of inhibitors with several therapeutic applications. In this connection, we report a new class of carbonic anhydrase inhibitors, based on the thiopyrano-fused pyrazole scaffold to which a pendant 4-sulfamoylphenyl moiety was attached. The new sulfonamides **3a−e** were designed as constrained analogues of celecoxib and valdecoxib. The most interesting feature of sulfonamides **3** was their predominantly strong inhibition of human (h) CA I and II, as well as those of the mycobacterial β-class enzymes (Rv1284, Rv3273, and Rv3588c), whereas their inhibitory action against hCA III, IV, VA, VB, VI, VII, IX, XII, XIII, and XIV was found to be at least 2 orders of magnitude lower. X-ray crystallography and structural superposition studies made it possible to explain the very distinct inhibition profile of the tricyclic sulfonamides, different from those of celecoxib and valdecoxib.

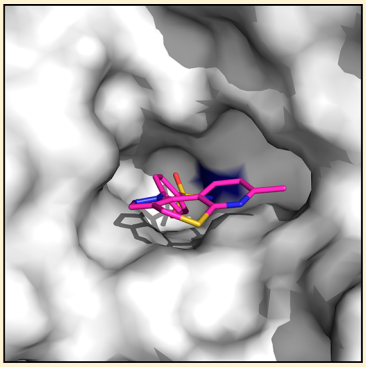

INTRODUCTION

The carbonic anhydrases (CAs, EC 4.2.1.1) are a superfamily of metalloenzymes which catalyze the interconversion between CO_2 and bicarbonate by using a metal hydroxide nucleophilic mechanism.[1−19] Five genetically distinct CA families are known to date, the α-, β-, γ-, δ-, and ζ-class enzymes.[1−6] They differ in their preference for the metal ion used within the active site for performing the catalysis as well as in the three-dimensional fold of the protein backbone, constituting a paradigmatic example of convergent Darwinian evolution at the molecular level. Zn(II) ions may be used by all five classes mentioned above, but the γ-CAs are probably Fe(II) enzymes (being active also with bound Zn(II) or Co(II) ions),[3,4] whereas the ζ-class uses Cd(II) or Zn(II) to perform the physiologic reaction catalysis.[5,6] The inhibition and activation of CAs are well understood processes, with most classes of inhibitors binding to the metal center[1−19] and activators binding at the entrance of the active site cavity. In this way, they participate in proton shuttling processes between the metal ion-bound water molecule and the environment, which is the rate-determining step in the catalytic cycle of most CA isoforms.[20,21] This process leads to the enhanced formation of the metal hydroxide, catalytically active species of the enzyme, shown in Scheme 1 (steps A−D). Inhibitors generally bind to the metal ion from the enzyme active site in the deprotonated state (as anions), as shown schematically in steps E and F of Scheme 1, for a tetrahedrally bound inhibitor (E) and for one in which the Zn(II) ion is in a trigonal bipyramidal geometry (F), a case in which a water molecule, in addition to the inhibitor, is also coordinated to Zn(II) ion (some inorganic anions bind in this way).[19] Although the mechanisms of Scheme 1 are depicted for an α-CA, they are valid even if another metal ion is present within the active site cavity, i.e., Cd(II) or Fe(II), as the corresponding hydroxides have similar nucleophilicity as the zinc hydroxide.[3−6] The same is true for a different coordination pattern of the metal ion (i.e., two Cys and one His residues), as for the β- and ζ-class CAs.[1−19] Sulfonamides and their bioisosteres (sulfamates, sulfamides),[1,2] representing the main class of pharmacologically relevant CA inhibitors (CAIs),[1−4] share with

Received: June 22, 2012
Published: October 15, 2012

Scheme 1. Catalytic and Inhibition Mechanisms (with Zinc Ion Binders) of α-CAs (hCA I Amino Acid Numbering of the Zinc Ligands)[a]

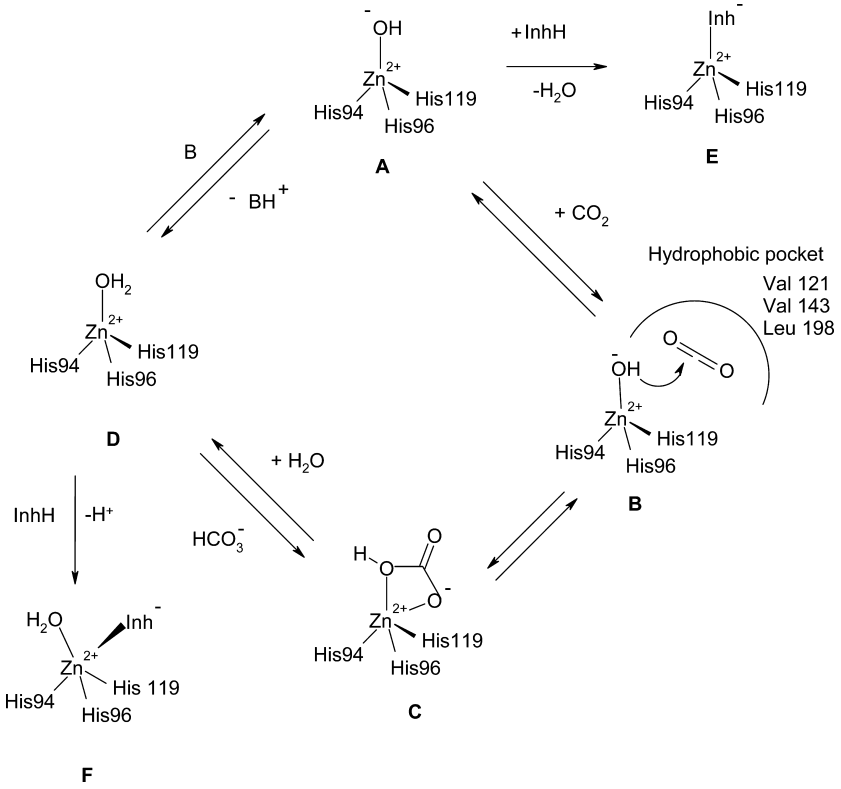

[a]A similar catalytic/inhibition mechanism is valid also for CAs from other classes (β-, γ-, and ζ-CAs), but either the metal ion is coordinated by other amino acid residues or a Cd(II) ion is present instead of zinc at the active site. Sulfonamides and dithiocarbamates bind as shown in step E.

dithiocarbamates[22−24] and some carboxylates[25−27] the inhibition mechanism depicted in step E.

It should be mentioned here that, recently, other CA inhibition mechanisms than the binding to the metal center were reported for α-CAs, which do not directly involve the metal ion from the enzyme active site.[28−33] For example, polyamines bind to the enzyme by anchoring to the zinc-coordinated water/hydroxide ion,[28] whereas coumarins act as prodrugs and bind at the entrance of the active site cavity, rather far away from the metal ion, after being hydrolyzed to 2-hydroxy-cinnamic acids.[29−33]

CA inhibition not only has pharmacological applications in the field of diuretics, antiglaucoma, anticonvulsant, and anticancer agents[1,2,7−11] but is also an emerging target for designing anti-infectives (antifungal and antibacterial agents)[34−36] with a novel mechanism of action. Sulfonamides, sulfamates, sulfamides, and dithiocarbamates belonging to many structural types were reported to possess significant inhibitory activities against many CA classes but were mostly investigated as inhibitors of the mammalian isoforms (16 of which are known in nonprimates and 15 in primates).[37,38]

Several drug design strategies have been reported ultimately based on the tail approach[39−42] for obtaining sulfonamides/dithiocarbamates, which exploit more external binding regions within the enzyme active site (in addition to coordination to the metal ion), thus leading to isoform-selective compounds.[43−47] The most promising data have been obtained by a combination of X-ray crystallography of enzyme−inhibitor adducts, with novel synthetic approaches for generating chemical diversity.[1,2,48−56] The exploration of novel scaffolds as well as high resolution X-ray crystallography of enzyme−inhibitor adducts may lead to novel classes of CAIs with the desired physicochemical and pharmacologic properties.

Continuing our research in the field, in this paper we explore for the first time tricyclic sulfonamides **3a−e** incorporating the poorly investigated benzothiopyrano[4,3-*c*]pyrazole (comp **3a−c**) and pyridothiopyrano[4,3-*c*]pyrazole (comp **3d−e**) systems, as well as the classical benzenesulfonamide moiety responsible for binding to the catalytically crucial metal ion.

Actually, the lead compounds used in the present drug design study were the clinically used derivatives celecoxib (**CLX**) and valdecoxib (**VLX**), initially launched as cyclooxygenase 2 (COX-2) specific inhibitors,[57−60] and later shown also to act as potent CAIs.[46,47,61] (Chart 1) Both compounds possess a benzenesulfonamide group linked to a five-membered, substituted heterocyclic ring. The presence of the SO_2NH_2 moiety seems not to be necessary for COX-2 inhibition, but it is essential for the CA inhibition.[46,47,57−60] The two compounds were shown to possess interesting and isoform-selective CA inhibitory action, and their X-ray crystal structures in complex with one human (h) CA isoform (hCA II) were reported by our group.[46,47] The rationale for designing the new compounds **3a−e** reported here was to use the benzenesulfonamide as a zinc binding moiety connected to a pyrazole moiety annealed with a bulky heterocyclic ring in order to explore both alternative chemotypes and the possibility to further enhance the isoform selectivity observed with celecoxib and valdecoxib as CAIs.[46,47,57−61] Furthermore, compounds **3a−e** may be regarded as geometrically constrained analogues of the two reference leads **CLX** and **VLX**.

dx.doi.org/10.1021/jm300878g | J. Med. Chem. 2012, 55, 9619−9629

Chart 1

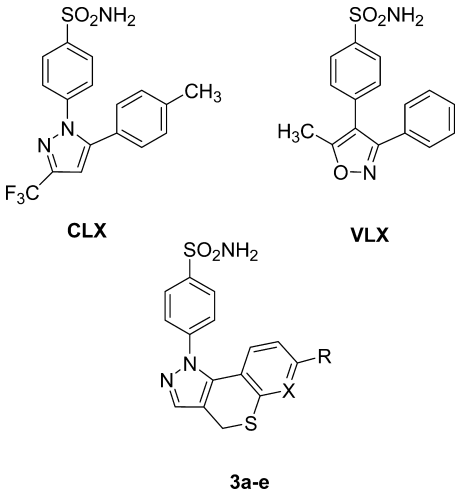

Compounds **3a–e** were investigated for the inhibition of 15 CAs of mammalian or bacterial origin, and one of them (**3e**) was crystallized in complex with hCA II, affording interesting hints for the drug design of sulfonamide CAIs belonging to this class of derivatives. Moreover, a possible dual activity on both COX-2 and CA isoforms was also assessed by an in vitro assay.

CHEMISTRY

The preparation of the 1-(*p*-sulfonamidophenyl) substituted pyrazole derivatives **3a–e** was performed following the synthetic route described in Scheme 2. The starting key intermediates 7-substituted-3-hydroxymethylenebenzothiopyranones **2a–c** or 3-hydroxymethylenepyrido thiopyranones **2d–e** were obtained by Claisen condensation of the appropriate thiopyranone **1a–e** with ethyl formate in toluene solution. Intermediates **1a–e** were prepared following previously described procedures.[62–64] Compounds **2a–b** and **2d–e** have been described earlier,[65–67] whereas **2c** was newly synthesized, following a similar procedure.[65–67] Analytical and IR, ^{1}H NMR spectral data of **2c** were in accordance with those of the analogous compounds **2a–b** and **2d–e**. Compounds **2a–e** have been obtained in good yields and sufficiently pure to be utilized in the second step of the synthetic procedure without crystallization. The condensation of **2a–e**, containing the reactive CH group adjacent to the C=O function, with *p*-sulfamidophenylhydrazine hydrochloride, afforded the new compounds **3a–e**, which were purified by crystallization. The purity of the target compounds was assessed by TLC analysis and by physicochemical properties, analytical, and ^{1}H NMR spectral data, which were in agreement with the proposed structures and with other previously reported results (see experimental protocols and Supporting Information Table 1 for details).[65–68]

RESULTS AND DISCUSSION

CA Inhibition. Compounds **3a–e** as well as the lead molecules **CLX** and **VLX** were assayed[69] as inhibitors of all catalytically active human CA isoforms, hCA I-XIV, and of the three mycobacterial *β*-class enzymes Rv1284, Rv3273, and Rv3588c, shown earlier to be interesting drug targets by our group[70–73] (Table 1). The following structure–activity relationship (SAR) can be evidenced from the data of Table 1:

i. The cytosolic, widespread isoforms hCA I and II were moderately (hCA I) or effectively (hCA II) inhibited by compounds **3**. The inhibition profile of these compounds, at least for hCA II, is quite similar to that of celecoxib and valdecoxib (Table 1), whereas the derivatives **3** were much better hCA I inhibitors compared to the lead compounds **CLX** and **VLX**. Indeed, the inhibition constants (K_Is) of **3a–e** against hCA I were in the range of 65–318 nM (versus 50–54 *μ*M for the lead molecules) and against hCA II in the range of 16–210 nM (versus 21–43 nM for **CLX** and **VLX**). The presence in the heterocyclic scaffold both of a benzene or a pyridine leads to effective CAIs. Moreover, the most effective inhibitors were those bearing the methoxy (**3a**) or chlorine (**3b**) as R moieties, while the CF_3 moiety as R substituent (**3c**) was associated with a lower inhibitory activity against both isoforms (Table 1).
ii. The cytosolic slow isoform hCA III was poorly inhibited by these sulfonamides, with K_Is in the range of 6.4–32.0 *μ*M, which are in the same range as for the coxibs **CLX** and **VLX**. This is probably due to the specific active site architecture of hCA III, which has a bulky Phe residue (Phe198) in the middle of the cavity, which interferes with the binding of sterically demanding compounds[74] such as **3a–e**.
iii. The membrane-anchored isoform hCA IV was moderately inhibited by compounds **3a–e**, with inhibition

Scheme 2. Synthesis of Sulfonamides 3a–e[a]

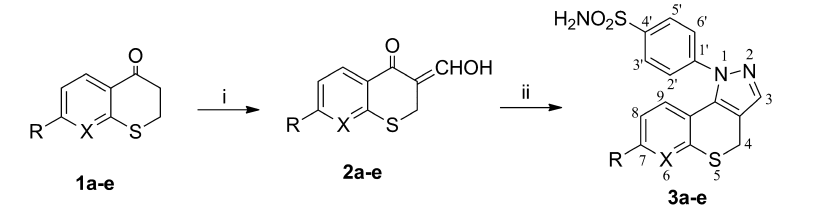

1a: X = CH R = OCH_3
1b: X = CH R = Cl
1c: X = CH R = CF_3
1d: X = N R = H
1e: X = N R = CH_3

2a: X = CH R = OCH_3
2b: X = CH R = Cl
2c: X = CH R = CF_3
2d: X = N R = H
2e: X = N R = CH_3

3a: X = CH R = OCH_3
3b: X = CH R = Cl
3c: X = CH R = CF_3
3d: X = N R = H
3e: X = N R = CH_3

[a]Reagents and conditions: (i) MeONa/MeOH, HCOOEt/anhydrous toluene, rt, 24 h N_2 atm; (ii) *p*-sulfonamidophenylhydrazine hydrochloride/refluxing methanol.

dx.doi.org/10.1021/jm300878g | J. Med. Chem. 2012, 55, 9619–9629

Table 1. Inhibition of hCA Isoforms I–XIV and Mycobacterial β-CAs Rv1284, Rv3273, and Rv3588c with Sulfonamides 3a–e, Celecoxib (CLX), and Valdecoxib (VLX) by a Stopped Flow CO_2 Hydrase Assay[69]

	K_I (nM)[a]						
enzyme	3a	3b	3c	3d	3e	CLX	VLX
hCA I	65	212	318	193	155	50000	54000
hCA II	16	29	210	72	49	21	43
hCA III	22700	32000	28600	6400	7900	7400	78000
hCA IV	8850	7200	7140	328	7500	880	1340
hCA VA	923	440	327	476	992	794	912
hCA VB	1072	3140	3250	3180	3270	93	88
hCA VI	7116	9280	9340	8055	8140	94	572
hCA VII	609	602	628	873	912	2170	3900
hCA IX	2182	1845	2570	2340	3250	16	27
hCA XII	4550	5620	6755	5540	5870	18	13
hCA XIII	938	2810	714	4300	4630	98	425
hCA XIV	931	797	548	715	844	689	107
Rv1284	870	412	613	134	115	10350	12970
Rv3273	750	316	238	286	241	7760	7810
Rv3588c	610	235	357	273	144	713	682

[a]Mean from three different assays. Errors were in the range of ±10 of the reported values (data not shown).

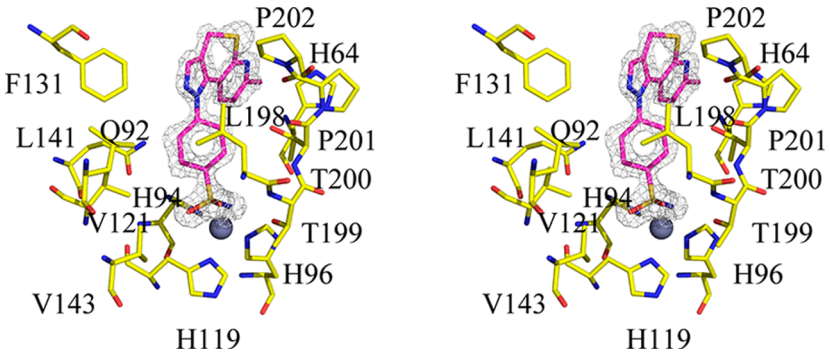

Figure 1. Stereo stick representation of hCA II active site complexed with **3e** (pink). The active-site zinc ion is depicted as a gray sphere. The electron density is represented by a 2σ-weighted $2F_o - F_c$ Fourier map (gray mesh). Amino acids are as labeled. Figure made using PyMOL (DeLano Scientific).

constants in the range of 328–8850 nM. The best CA inhibitor was **3d**, which incorporates the 7-unsubstituted pyridine ring (R = H).

iv. The mitochondrial isoforms hCA VA and VB, as well as the secreted one hCA VI, were inhibited by these compounds and by the coxibs, with inhibition constants in the range of 327–9340 nM (Table 1). Among these isoforms, hCA VA was the mostly inhibited, followed by hCA VB and hCA VI. Actually, this may be a useful inhibition pattern, because many sulfonamide drugs have side effects due to the inhibition of the secreted, salivary (hCA VI), or mitochondrial enzymes (hCA VA and VB).[75]

v. The remaining cytosolic isoforms, hCA VII and XIII, were also moderately inhibited by the new compounds **3**, with K_Is in the range of 602–912 nM against hCA VII, and of 714–4630 nM against hCA XIII, respectively (Table 1). Against hCA VII, the benzo-fused derivatives **3a–c** had similar inhibitory activity, whereas the two pyrido-fused derivatives **3d–e** were CAIs slightly less effective on this isoform. It seems that for this isoform the nature of the R moiety has less influence on the inhibitory action. On the contrary, against hCA XIII this seems to be the most important parameter influencing activity, with compound **3c** (R = CF_3) showing the best inhibition values. It should be also noted that the coxibs **CLX** and **VLX** are weak hCA VII inhibitors but show a significantly better inhibition profile against hCA XIII.

vi. The transmembrane isoforms hCA IX, XII and XIV were modestly inhibited by the new compounds **3a–e**, which usually showed an activity in the low micromolar–submicromolar range. hCA XIV was the isoform more prone to be inhibited by the compounds (K_Is in the range of 548–931 nM), followed by hCA IX (K_Is in the range of 1845–3250), with hCA XII that was the least inhibited one (K_Is in the range of 4550–6755 nM).

vii. The newly investigated compounds **3a–e** showed relevant inhibition profiles also toward the mycobacterial enzymes Rv1284, Rv3273, and Rv3588c (Table 1). For example, Rv1284 was inhibited with K_Is in the range of 115–870 nM. It is interesting to note that the two pyridine incorporating compounds **3d** and **3e** were much more effective than the benzene analogues **3a–c**. The same behavior has been also observed in the inhibition assays of the remaining mycobacterial enzymes, Rv3273 and Rv3588c (Table 1). Indeed, the last two compounds, **3d** and **3e**, had K_Is in the range of 241–286 nM against Rv3273 and of 144–273 nM against Rv3588c,

dx.doi.org/10.1021/jm300878g | J. Med. Chem. 2012, 55, 9619–9629

respectively. However, it has to be pointed out that also the benzothiopyrano derivatives **3b** and **3c** showed significative inhibitory activities against each of these enzymes: Rv3588c (K_I of 235 nM) and Rv3272 (K_I of 238 nM), respectively.

X-ray Crystallography. To better understand inhibition of CAs with these compounds, X-ray crystallographic studies were performed on **3e** in complex with hCA II. The crystal structure was determined to 1.5 Å resolution, using protocols previously described,[76,77] **3e** refined with an occupancy of 0.80, and *B*-factors that were comparable to the solvent within the active site. Residual density adjacent to **3e** was observed in the final $F_o - F_c$ electron density map, revealing a possible second conformer, but refinement efforts to fit this weaker binding site were unsuccessful as the electron density was too diffuse to fit a reliable ordered second molecule. **3e** was buried deep into the active site and displaced the catalytic zinc-bound solvent, such that the sulfonamide nitrogen was bound directly to the zinc ion (distance ∼2.0 Å). The N and O2 atoms of the sulfonamide were also within hydrogen bond distances (2.9−3.0 Å) of OG1 and N of Thr199. This observation is consistent with the results of the other sulfonamide inhibitors complexed to CAs investigated so far.[76−80] The sulfur atom caused a pucker in the ring geometry but was not directly involved in any interaction with hCA II. Protruding out of the active site, the inhibitor's hydrophobic rings were stabilized predominantly by hydrophobic residues that line the active site cavity, engaging good van der Waals interactions with the side chains of Val121, Phe131, Leu198, Pro202, and His64 (the proton shuttle residue of hCA II). **3e** was buried within the active site with 407 Å^2 (78.1%) of its surface area in contact with hCA II (Figure 1). The crystallographic parameters and data collection statistics are shown in Table 2.

The superposition of the hCA II−**3e** structure was carried out with celecoxib (**CLX**, PDB: 1OQ5)[46] and valdecoxib (**VLX**, PDB: 2AW1),[47] also in complex with hCA II using Coot.[81] The most striking feature of this comparison, given that all the inhibitors are tethered to the active site zinc, is the capacity of their tail groups to occupy very different surface locations of the active site (Figure 2). Notably, the hydrophobic phenyl ring of the ligand **VLX** pushes the Phe131 out of the hydrophobic pocket compared to inhibitors **3e** and **CLX** (Figure 2B compared to parts A and C). In a similar manner, the pendant hydrophobic phenyl ring of **CLX** forces Asn67 to change conformation differently from inhibitors **3e** and **VLX** (Figure 2C compared to parts A and B). In addition, **CLX** has both a fluorine rich hydrophilic region and a hydrophobic phenyl ring at its terminus. Interestingly, the fluorine rich group is located in the hydrophilic pocket (Leu204, Pro202, Phe131, and Val135) and the hydrophobic phenyl ring is positioned in the hydrophilic pocket (Asn62, Asn67, Glu69, and Gln92). This unusual orientation could be attributed to the bulky nature of the ligand, bearing a large phenyl group in the 5-position of the heterocyclic ring, which may cause a steric hindrance in the relatively small hydrophobic pocket in the active site of hCA II (Figure 2B). On the other hand, the hydrophilic nitrogen atom in the fused pyridine ring of **3e** may be involved in hydrogen bonding with the bulk solvent and hence does not need to stay in the Phe131 hydrophobic pocket. Despite the different conformational changes in hCA II side chains induced by the ligand binding (Figure 2) and their distinctly different orientations within the active site (Figure 2), all three inhibitors, **3e**, **CLX**, and **VLX** bury approximately the same amount of surface area of the protein: 407, 451, and 409 Å^2 respectively.

Table 2. Crystallographic Data Refinement and Model Statistics of the hCA II−3e Adduct

	3e
PDB accession	3QYK
Data Collection Statistics	
temperature (K)	100
wavelength (Å)	1.5418
space group	$P2_1$
unit cell parameters (Å)	a = 42.3
	b = 41.4
	c = 72.3
	β = 104.2
no. of unique reflections	39832
resolution (Å)	50.0−1.4 (1.52−1.47)[e]
R_{sym}[a] (%)	5.6 (19.0)
$I/\sigma(I)$	23.75 (7.2)
completeness	96.0 (92.0)
redundancy	4.9 (4.8)
Final Model Statistics	
R_{cryst}[b] (%)	0.157
R_{free}[c] (%)	0.177
residue numbers	4−261
no. of protein atoms[d]	2288
no. of drug atoms	24
no. of H_2O molecules	265
rmsd bond lengths (Å)	0.01
rmsd bond angles (deg)	1.40
Ramachandran statistics (%): Most favored, allowed, and outliers	88.4, 11.6, 0.0
average *B* factors (Å^2): main chain, side chain, compound, solvent	12.1, 14.9, 13.3, 29.2

[a] $R_{sym} = \sum |I - \langle I \rangle| / \sum \langle I \rangle$. [b] $R_{cryst} = (\sum ||F_o| - |F_c|| / \sum |F_{obs}|) \times 100$. [c] R_{free} is calculated in same manner as R_{cryst}, except that it uses 5% of the reflection data omitted from refinement. [d] Includes alternate conformations. [e] Values in parentheses represent highest resolution bin.

Structural Superposition. The crystal structure determination of **3e** complexed to hCA II raised several other questions related to the CAI's specificity. Although the overall structures of hCA I, II, IX, and XII are similar, compound **3e** behaves as a highly effective hCA I and II inhibitor, with reduced affinity against hCA IX and XII (Table 1). To investigate the reasons of such binding profile, the crystal structures of hCA I (PDB ID: 2NMX),[82] hCA IX (PDB ID: 3IAI),[83] and hCA XII (PDB ID: 1JCZ)[84] were superimposed with the structure of hCA II in complex with **3e** (PDB ID: 3QYK), highlighting that the differences in affinities could be attributed to a reduction in hydrophobicity in the hydrophobic pockets within the active sites of hCA IX and XII. Namely, Val131 and Ala204 in hCA IX and Ala131 and Asn204 in hCA XII cause a decrease in hydrophobicity compared to their equivalent amino acids in hCA I and II (Figure 3A, Table 3). Moreover, Arg62 in hCA IX, and residues Lys67, Thr91, Ser135, and Asn204 in hCA XII impart hydrophilic properties to the otherwise hydrophobic region in hCA I and hCA II (Figure 3B, Table 3). hCA II (PDB ID: 3QYK) had an rmsd (main chain) of 0.86 Å with hCA I (PDB ID: 2NMX),[82] 1.52 Å with hCA IX (PDB ID: 3IAI),[83] and 1.14 Å with hCA XII (PDB ID: 1JCZ).[84]

dx.doi.org/10.1021/jm300878g | J. Med. Chem. 2012, 55, 9619−9629

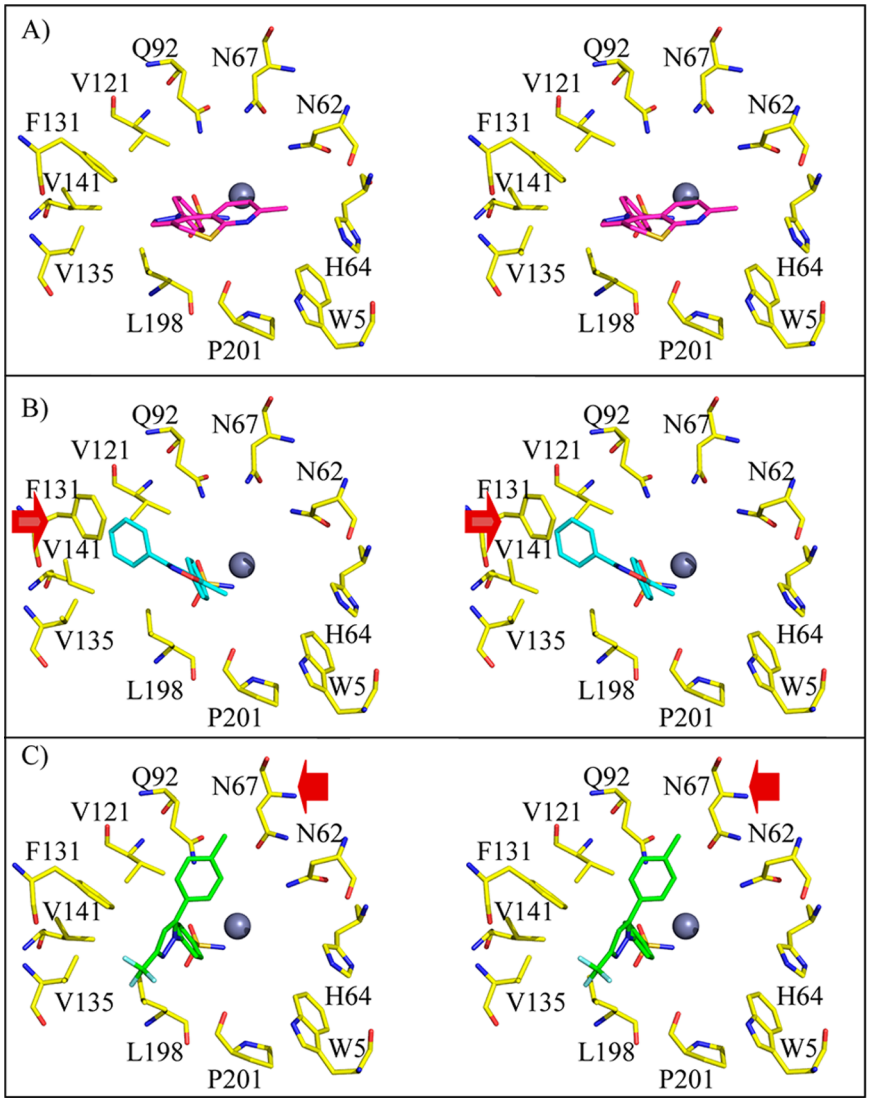

Figure 2. Stick figure of inhibitors (A) **3e** (pink), (B) valdecoxib **VLX** (cyan), and (C) celecoxib **CLX** (green), superimposed on the active site of hCA II. View looking into the active site of hCA II. Amino acids are depicted in yellow sticks as labeled. The active-site zinc is represented as a gray sphere. Red solid arrows indicate hCA II conformational change on inhibitor binding. Figure made using PyMOL (DeLano Scientific).

Similarly, the binding affinities of compound **3e** toward hCA I and II, different from those of the reference compounds **CLX** and **VLX**, were investigated at molecular level. The inhibition data show that compound **3e** is a better inhibitor of hCA I than **CLX** and **VLX**, although they bind with similar affinities with hCA II. This can be attributed to the reason that residue His67 in hCA I (PDB ID: 2NMX),[82] in place of Asn67 in hCA II, has fewer degrees of conformational freedom and therefore causes a steric clash with **CLX**. The possible rotamers of His67 were examined, but none allowed the binding of **CLX** without a steric clash. Conversely, compound **3e** binds in a different orientation within the active site and hence His67 does not affect its binding (Figure 4). Regarding **VLX**, when modeled into hCA I, it is surrounded by residues that are different from those of hCA II, and this difference in the environment could be a potential reason for the difference in its inhibition constants. Residues Ala121, Phe91, and Leu131 in hCA I, in place of Val, Ile, and Phe in hCA II, have a slightly reduced hydrophobicity and Leu131 seems to cause a putative clash with **VLX**. These differences in amino acid residues do not affect compound's **3e** binding due to its different orientation within the active site (Figure 5).

A complete listing of amino acid differences that may contribute to the effect on the binding affinities of the compounds with hCA I, II, IX and XII, is reported in Table 3.

COX-2 Inhibition. As mentioned above, both reference sulfonamido-type coxibs, **CLX** and **VLX**, demonstrate action as potent inhibitors of several CA isoforms, with activities in the same order of magnitute as those of clinically used CAIs.[46,47,61] This inhibition profile suggested that also our sulfonamide containing derivatives **3a–e** might possess COX-2 inhibition properties, thus, the inhibitory activity of compounds **3a–e** against ovine COX-2 was determined. The inhibitory effect of the new derivatives was routinely estimated at a concentration of 100 μM by the Colorimetric COX inhibitor screening assay, which exploits the peroxidase component of cyclooxygenases.[85] None of the assayed compound showed any inhibitory effect (data not shown).

Consistent with these results, the newly investigated compounds **3a–e** demonstrated to behave as CAs selective inhibitors.

dx.doi.org/10.1021/jm300878g | J. Med. Chem. 2012, 55, 9619–9629

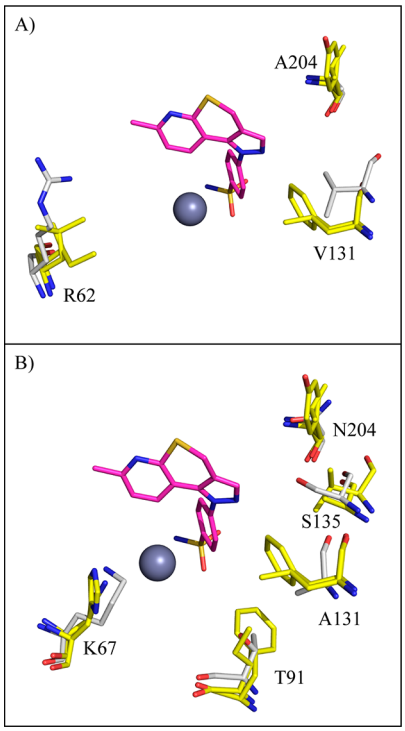

Figure 3. Stick representation of compound **3e** (pink) shown in the active sites of hCA I (yellow, PDB ID: 2NMX[82]) and hCA II (yellow, PDB ID: 3QYK) compared with (A) hCA IX (PDB ID: 3IAI[83]) amino acids labeled (gray) and (B) hCA XII (PDB ID: 1JCZ[84]) amino acids labeled (gray). Compare with Table 3. hCA II numbering. Zn is shown as a gray sphere. Figure made using PyMOL (DeLano Scientific).

Table 3. Amino Acid Differences in the Active Site of hCA I, II, IX, and XII (hCA II Numbering)

residue no.	CA I	CA II	CA IX	CA XII
62	Val	Asn	Arg	Asn
67	His	Asn	Gln	Lys
91	Phe	Ile	Leu	Thr
121	Ala	Val	Val	Val
131	Leu	Phe	Val	Ala
135	Ala	Val	Leu	Ser
204	Tyr	Leu	Ala	Asn

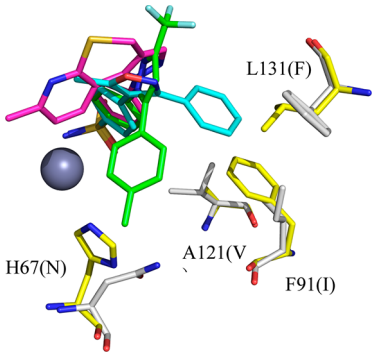

Figure 4. Stick representation of compounds **3e** (pink), celecoxib **CLX** (green), and valdecoxib **VLX** (cyan shown in the active sites of hCA I (yellow) compared with hCA II (gray). Note for hCA I His67 and Leu131 can cause a putative clash with **CLX** and **VLX**, respectively. hCA II amino acid in parentheses. Zn is shown as a gray sphere. Figure made using PyMOL (DeLano Scientific).

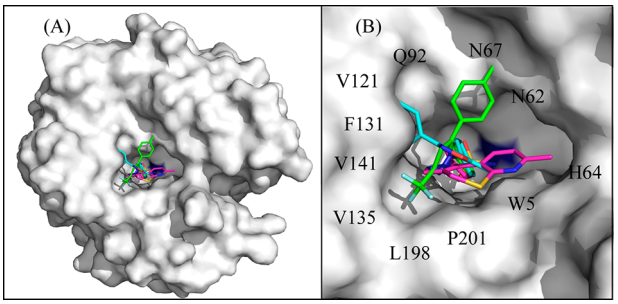

Figure 5. (A) Surface view of inhibitors **3e** (pink), celecoxib **CLX** (green), and valdecoxib **VLX** (cyan) superimposed in the active site of hCA II. hCA II is depicted as a surface representation (gray), and the zinc is depicted as a blue surface. (B) close-up of the active site. Amino acids are as labeled. Figure made using PyMOL (DeLano Scientific).

CONCLUSIONS

The ubiquitous metallo-enzymes CAs play important functions in crucial processes connected with respiration and CO_2/bicarbonate transport between metabolizing tissues and lungs, thus affecting many physiological or pathological events. This can explain why several inhibitors, CAIs, of these enzymes are clinically efficient agents, marketed as antiglaucoma, diuretic, or antiepilectic drugs. In addition, besides the α-class CAs, the β-CAs are the most abundant catalysts in metabolically diverse species such as bacteria or pathogenic fungi, thus becoming the potential target of CAI-based antibiotics/antifungals.

The whole CAIs group includes a number of structurally related agents whose most distinctive feature is a sulfonamido moiety responsible for the coordination bond to the Zn^{2+} ion of the enzymes. On the basis of the above considerations, we investigated a new class of CAIs based on the benzo- or pyrido-fused thiopyrano[4,3-*c*]pyrazole scaffold, characterized by a pendant 4-sulfamoylphenyl moiety. The new compounds **3a−e**, obtained by an original synthesis, have been designed by using as lead molecules the CAIs celecoxib and valdecoxib, both possessing an arylsulfonamide group in their structure. The most interesting feature of this new class of sulfonamides was their capacity to predominantly exert strong inhibition of only hCA I and II, as well as of the mycobacterial β-class enzymes (Rv1284, Rv3273, and Rv3588c), whereas their inhibitory activity against hCA III, IV, VA, VB, VI, VII, IX, XII, XIII, and XIV was at least 2 orders of magnitude lower. The combination of X-ray crystal structure of the hCAII−compound **3e** adduct, and homology modeling allowed to explain this peculiar inhibition profile, which is also quite different from those of the reference coxibs, **CLX** and **VLX**. Thus, the benzenesulfonamides **3a−e** constitute a highly interesting class of compounds which, inhibiting only a restricted number of physiologically relevant CA isoforms among the 12 catalytically active human such enzymes, should lead to fewer side effects. In addition, the good inhibition profile of some of the new derivatives (**3d−e**) against mycobacterial CAs is also to be considered as relevant because these enzymes are less inhibited by other classes of sulfonamides.

Finally, the sulfonamido type CAIs **CLX** and **VLX** are known to act also as potent COX-2 inhibitors, with serious concerns about their cardiovascular side effects. Consequently, the high selectivity toward hCA isoforms of compounds **3a−e**, which do not show any inhibitory activity against COX-2, may be regarded as an important clinical advantage.

dx.doi.org/10.1021/jm300878g | *J. Med. Chem.* 2012, 55, 9619−9629

EXPERIMENTAL SECTION

Chemistry. The uncorrected melting points were determined using a Reichert Köfler hot-stage apparatus. IR spectra were obtained on a NICOLET/AVATAR 360 FT spectrophotometer by Nujol mulls. ^{1}H NMR spectra were recorded on a Varian Gemini 200 spectrometer in dimethyl-d_6 sulfoxide solution. The coupling constants are given in Hertz. Elemental analyses were performed by our Analytical Laboratory and were within ±0.4%. Magnesium sulfate was used as the drying agent. Evaporations were made in vacuo (rotating evaporator). Analytical TLC were carried out on Merck 0.2 mm precoated silica gel aluminum sheets (60 F-254). Reagents, starting materials, and solvents were purchased from commercial suppliers and used as received. According to the methods described previously, the following substrates were obtained: 7-trifluoromethyl-2,3-dihydro-4*H*-1-benzothiopyran-4-one (**1c**),[63] 7-methoxy- (**2a**) and 7-chloro- (**2b**) 2,3-dihydro-3-hydroxymethylene-1-benzothiopyran-4(4*H*)-ones,[65] 2,3-dihydro-3-hydroxymethylenethiopyrano[2,3-*b*]pyridin-4(4*H*)-one (**2d**),[67] 7-methyl-2,3-dihydro-3-hydroxymethylenethiopyrano[2,3-*b*]-pyridin-4(4*H*)-one (**2e**).[65] The preparation of compound 7-trifluoromethyl-2,3-dihydro-3-hydroxymethylene-1-benzothiopyran-4(4*H*)-one (**2c**) is described in Supporting Information.

7-Substituted-1-(*p*-sulfonamidophenyl)-1,4-dihydrobenzothiopyrano[4,3-*c*]pyrazoles 3a−c and 7-Substituted-1-(*p*-sulfonamidophenyl)-1,4-dihydro-pyrido[3′,2′:5,6]-thiopyrano [4,3-*c*]pyrazoles 3d−e. *General Procedure.* *p*-Sulfonamidophenylhydrazine hydrochloride (5.40 mmol) was added to a solution of the appropriate hydroxymethylene derivative **2a−e** (4.50 mmol) in 50 mL of methanol, and the reaction mixture was stirred at room temperature for 24 h and then refluxed for 7 h. After cooling, the yellow solid, when present, was collected and the solution was evaporated under reduced pressure. The solid and the residue were washed with an aqueous potassium carbonate saturated solution to give crude pyrazoles **3a−e**, which were purified by crystallization from ethanol (see Supporting Information Tables 1−2 for physical, analytical, and spectral data).

CA Inhibition. An Applied Photophysics stopped-flow instrument has been used for assaying the CA catalyzed CO_2 hydration activity. Phenol red (at a concentration of 0.2 mM) has been used as indicator, working at the absorbance maximum of 557 nm, with 20 mM Hepes/TRIS (pH 7.5 for α-CAs, and 8.4, for β-CAs) as buffer and 20 mM Na_2SO_4 (for maintaining constant the ionic strength), following the initial rates of the CA-catalyzed CO_2 hydration reaction for a period of 10−100 s.[69] The CO_2 concentrations ranged from 1.7 to 17 mM for the determination of the kinetic parameters and inhibition constants. For each inhibitor, at least six traces of the initial 5−10% of the reaction have been used for determining the initial velocity. The uncatalyzed rates were determined in the same manner and subtracted from the total observed rates. Stock solutions of inhibitor (0.1 mM) were prepared in distilled−deionized water, and dilutions up to 0.01 nM were done thereafter with the assay buffer. Inhibitor and enzyme solutions were preincubated together for 15 min at room temperature prior to assay in order to allow for the formation of the E−I complex. The inhibition constants were obtained by nonlinear least-squares methods using PRISM 3, as reported earlier,[22−24] and represent the mean from at least three different determinations. All CA isofoms were recombinant ones obtained in house as reported earlier.[29,30,70−73]

X-ray Crystal Structure Determination. Co-crystals for the hCA II−**3e** complex were obtained using the hanging drop vapor diffusion method.[86] Drops of 10 μL (0.4 mM hCA II, 0.8 mM **3e**, 0.1% dimethyl sulfoxide (DMSO), 0.8 M sodium citrate, 50 mM Tris-HCl, pH 7.8) were equilibrated against the precipitant solution (1.6 M sodium citrate; 50 mM Tris-HCl; pH 7.8) at room temperature (~20 °C). Crystals were observed after 5 days. A crystal was cryoprotected by quick immersion into 20% sucrose precipitant solution and flash-cooled by exposing to a gaseous stream of nitrogen at 100 K. The X-ray diffraction data was collected using an R-AXIS IV^{+2} image plate system on a Rigaku RU-H3R Cu rotating anode operating at 50 kV and 22 mA, using Osmic Varimax HR optics. The detector−crystal distance was set to 76 mm. The oscillation steps were 1° with a 5 min exposure per image. Indexing, integration, and scaling were performed using HKL2000.[87] Starting phases were calculated from Protein Data Bank entry 3KS3[88] with waters removed. Refinement using Phenix package,[89] with 5% of the unique reflections selected randomly and excluded from the refinement data set for the purpose of R_{free} calculations, was alternated with manual refitting of the model and solvent placement in Coot.[81] The validity of the final model was assessed by PROCHECK.[90] Complete refinement statistics and model quality are included in Table 2.

Structural Superposition. To compare the differences in amino acid residues (among four isoforms of hCA) involved in interactions with **3e**, the crystal structure of hCA II in complex with **3e** (PDB ID: 3QYK) was superposed with highest resolution (1.5 Å) crystal structure of hCA I (PDB ID: 2NMX),[82] the only available crystal structure of hCA IX (PDB ID: 3IAI)[83] and the only uncomplexed crystal structure available of hCA XII (PDB ID: 1JCZ),[84] using the Secondary Structure Matching (SSM) tool in Coot.[81] Additionally, to investigate the differential binding of **CLX** and **VLX** (as compared to **3e**) with hCA I and hCA II, the crystal structures of hCA II in complex with **CLX** (PDB ID: 1OQ5),[46] **VLX** (PDB ID: 2AW1),[47] and **3e** (PDB ID: 3QYK) were superposed with hCA I (2NMX).[82]

COX-2 Inhibitory Assay. The inhibitory activity of compounds **3a−e** against ovine COX-2 was determined by the Colorimetric COX inhibitor screening assay. Ovine COX-2 and Colorimetric COX inhibitor screening assay, catalogue no. 760111, were from Cayman Chemical (Ann Arbor, MI, USA). Test compounds **3a−e** (2.2 mM, 10 μL) were incubated at 25 °C for 5 min and under shaking, with ovine COX-2 enzyme solution (10 μM), heme (10 μL), and assay buffer (0.1 M Tris-HCl, pH 8, 150 μL). Arachidonic acid (20 μL) and the colorimetric substrate solution (*N*,*N*,*N*′,*N*′-tetramethyl-*p*-phenylenediamine, TMPD, 20 μL) were then added, and the resulting mixture was incubated at 25 °C for 5 min. At the end, the residual activity of COX-2 enzyme was determined colorimetrically by monitoring the appearance of the oxidized TMPD, measured at 590 nm with a PerkinElmer Lambda 25.

All the test compounds **3a−e** were dissolved into dilute assay buffer, and their solubility was facilitated by using DMSO, whose concentration never exceeded 5% in the final reaction mixture. The inhibitory effect of the derivatives was routinely estimated at a concentration of 100 μM.

ASSOCIATED CONTENT

Supporting Information

Synthetic procedure of compound **2c**. Tables including physical, analytical, and spectral data of compounds **2c** and **3a−e**. This material is available free of charge via the Internet at http://pubs.acs.org.

AUTHOR INFORMATION

Corresponding Author

*Phone: +39 050 2219555. Fax: +39 050 2219605. E-mail: marini@farm.unipi.it.

Notes

The authors declare no competing financial interest.

ACKNOWLEDGMENTS

This research was financed in part by a grant of the 7th Framework Programme of the European Union (METOXIA project).

ABBREVIATIONS USED

CAs, carbonic anhydrases; hCAII, human carbonic anhydrase isoform II; CAIs, carbonic anhydrase inhibitors; CLX, celecoxib; VLX, valdecoxib; COX-2, cyclooxygenase-2

REFERENCES

(1) Alterio, V.; Di Fiore, A.; D'Ambrosio, K.; Supuran, C. T.; De Simone, G. Multiple binding modes of inhibitors to carbonic anhydrases: how to design specific drugs targeting 15 different isoforms? *Chem. Rev.* **2012**, *112*, 4421−4468.

(2) Supuran, C. T. Carbonic anhydrases: novel therapeutic applications for inhibitors and activators. *Nature Rev. Drug Discovery* **2008**, *7*, 168−181.

(3) Smith, K. S.; Jakubzick, C.; Whittam, T. S.; Ferry, J. G. Carbonic anhydrase is an ancient enzyme widespread in prokaryotes. *Proc. Natl. Acad. Sci. U.S.A.* **1999**, *96*, 15184−15189.

(4) Zimmerman, S. A.; Ferry, J. G.; Supuran, C. T. Inhibition of the Archaeal β-Class (Cab) and γ-Class (Cam) Carbonic Anhydrases. *Curr. Top. Med. Chem.* **2007**, *7*, 901−908.

(5) Xu, Y.; Feng, L.; Jeffrey, P. D.; Shi, Y.; Morel, F. M. Structure and metal exchange in the cadmium carbonic anhydrase of marine diatoms. *Nature* **2008**, *452*, 56−61.

(6) Alterio, V.; Langella, E.; Viparelli, F.; Vullo, D.; Ascione, G.; Dathan, N. A.; Morel, F. M. M.; Supuran, C. T.; De Simone, G.; Monti, S. M. Structural and inhibition insights into carbonic anhydrase CdCA1 from the marine diatom *Thalassiosira weissflogii*. *Biochimie* **2012**, *94*, 1232−1241.

(7) Ahlskog, J. K.; Schliemann, C.; Mårlind, J.; Qureshi, U.; Ammar, A.; Pedleym, R. B.; Neri, D. In vivo targeting of tumor-associated carbonic anhydrases using acetazolamide derivatives. *Bioorg. Med. Chem. Lett.* **2009**, *19*, 4851−4856.

(8) Neri, D.; Supuran, C. T. Interfering with pH regulation in tumours as a therapeutic strategy. *Nature Rev. Drug Discovery* **2011**, *10*, 767−777.

(9) Supuran, C. T. Carbonic anhydrase inhibitors. *Bioorg. Med. Chem. Lett.* **2010**, *20*, 3467−3474.

(10) Pastorekova, S; Parkkila, S; Pastorek, J; Supuran, C. T. Carbonic anhydrases: current state of the art, therapeutic applications and future prospects. *J. Enzyme Inhib. Med. Chem.* **2004**, *19*, 199−229.

(11) Supuran, C. T. Structure-based drug discovery of carbonic anhydrase inhibitors. *J. Enzyme Inhib. Med. Chem.* **2012**, DOI: 10.3109/14756366.2012.672983.

(12) Domsic, J. F.; Avvaru, B. S.; Kim, C. U.; Gruner, S. M.; Agbandje-McKenna, M.; Silverman, D. N.; McKenna, R. Entrapment of carbon dioxide in the active site of carbonic anhydrase II. *J. Biol. Chem.* **2008**, *283*, 30766−30771.

(13) Maupin, C. M.; Castillo, N.; Taraphder, S.; Tu, C.; McKenna, R.; Silverman, D. N.; Voth, G. A. Chemical rescue of enzymes: proton transfer in mutants of human carbonic anhydrase II. *J. Am. Chem. Soc.* **2011**, *133*, 6223−6234.

(14) Suarez Covarrubias, A.; Larsson, A. M.; Hogbom, M.; Lindberg, J.; Bergfors, T.; Bjorkelid, C.; Mowbray, S. L.; Unge, T.; Jones, T. A. Structure and function of carbonic anhydrases from *Mycobacterium tuberculosis*. *J. Biol. Chem.* **2005**, *280*, 18782−18789.

(15) Suarez Covarrubias, A.; Brgfors, T.; Jones, T. A.; Hogbom, M. Structural mechanics of the pH-dependent activity of the β-carbonic anhydrase from *Mycobacterium tuberculosis*. *J. Biol. Chem.* **2006**, *281*, 4993−4999.

(16) Supuran, C. T. Carbonic anhydrase inhibitors and activators for novel therapeutic applications. *Future Med. Chem.* **2011**, *3*, 1165−1180.

(17) Supuran, C. T.; Scozzafava, A.; Casini, A. Carbonic anhydrase inhibitors. *Med. Res. Rev.* **2003**, *23*, 146−189.

(18) Baranauskiene, L.; Hilvo, M.; Matuliene, J.; Golovenko, D.; Manakova, E.; Dudutiene, V.; Michailoviene, V.; Torresan, J.; Jachno, J.; Parkkila, S.; Maresca, A.; Supuran, C. T.; Grazulis, S.; Matulis, D. Inhibition and binding studies of carbonic anhydrase isozymes I, II and IX with benzimidazo[1,2-*c*][1,2,3]thiadiazole-7-sulphonamides. *J. Enzyme Inhib. Med. Chem.* **2010**, *25*, 863−870.

(19) Huang, S.; Hainzl, T.; Grundström, C.; Forsman, C.; Samuelsson, G.; Sauer-Eriksson, A. E. Structural studies of β-carbonic anhydrase from the green alga *Coccomyxa*: inhibitor complexes with anions and acetazolamide. *PLoS One* **2011**, *6*, e28458.

(20) Briganti, F.; Mangani, S.; Orioli, P.; Scozzafava, A.; Vernaglione, G.; Supuran, C. T. Carbonic anhydrase activators: X-ray crystallographic and spectroscopic investigations for the interaction of isozymes I and II with histamine. *Biochemistry* **1997**, *36*, 10384−10392.

(21) Temperini, C.; Scozzafava, A.; Vullo, D.; Supuran, C. T. Carbonic anhydrase activators. Activation of isozymes I, II, IV, VA, VII and XIV with L- and D-histidine and crystallographic analysis of their adducts with isoform II: engineering proton transfer processes within the active site of an enzyme. *Chemistry* **2006**, *12*, 7057−7066.

(22) Carta, F.; Aggarwal, M.; Maresca, A.; Scozzafava, A.; McKenna, R.; Supuran, C. T. Dithiocarbamates: a new class of carbonic anhydrase inhibitors. Crystallographic and kinetic investigations. *Chem. Commun.* **2012**, *48*, 1868−1870.

(23) Monti, S. M.; Maresca, A.; Carta, F.; De Simone, G.; Mühlschlegel, F. A.; Scozzafava, A.; Supuran, C. T. Dithiocarbamates strongly inhibit the beta-class fungal carbonic anhydrases from *Cryptococcus neoformans*, *Candida albicans* and *Candida glabrata*. *Bioorg. Med. Chem. Lett.* **2012**, *22*, 859−862.

(24) Carta, F.; Aggarwal, M.; Maresca, A.; Scozzafava, A.; McKenna, R.; Masini, E.; Supuran, C. T. Dithiocarbamates Strongly Inhibit Carbonic Anhydrases and Show Antiglaucoma Action in Vivo. *J. Med. Chem.* **2012**, *55*, 1721−1730. (b) Kolayli, S.; Karahalil, F.; Sahin, H.; Dincer, B.; Supuran, C. T. Characterization and inhibition studies of an α-carbonic anhydrase from the endangered sturgeon species *Acipenser gueldenstaedti*. *J. Enzyme Inhib. Med. Chem.* **2011**, *26*, 895−900.

(25) De Simone, G.; Supuran, C. T. (In)organic anions as carbonic anhydrase inhibitors. *J. Inorg. Biochem.* **2012**, *111*, 117−129.

(26) Parkkila, S.; Vullo, D.; Maresca, A.; Carta, F.; Scozzafava, A.; Supuran, C. T. Serendipitous fragment-based drug discovery: ketogenic diet metabolites and statins effectively inhibit several carbonic anhydrases. *Chem. Commun.* **2012**, *48*, 3551−3553.

(27) Temperini, C.; Scozzafava, A.; Supuran, C. T. Carbonic anhydrase inhibitors. X-Ray crystal studies of the carbonic anhydrase II—trithiocarbonate adduct—An inhibitor mimicking the sulfonamide and urea binding to the enzyme. *Bioorg. Med. Chem. Lett.* **2010**, *20*, 474−478.

(28) Carta, F.; Temperini, C.; Innocenti, A.; Scozzafava, A.; Kaila, K.; Supuran, C. T. Polyamines inhibit carbonic anhydrases by anchoring to the zinc-coordinated water molecule. *J. Med. Chem.* **2010**, *53*, 5511−5522.

(29) Maresca, A.; Temperini, C.; Vu, H.; Pham, N. B.; Poulsen, S. A.; Scozzafava, A.; Quinn, R. J.; Supuran, C. T. Non-zinc mediated inhibition of carbonic anhydrases: coumarins are a new class of suicide inhibitors. *J. Am. Chem. Soc.* **2009**, *131*, 3057−3062.

(30) Maresca, A.; Temperini, C.; Pochet, L.; Masereel, B.; Scozzafava, A.; Supuran, C. T. Deciphering the mechanism of carbonic anhydrase inhibition with coumarins and thiocoumarins. *J. Med. Chem.* **2010**, *53*, 335−344.

(31) Maresca, A.; Supuran, C. T. Coumarins incorporating hydroxy- and chloro- moieties selectively inhibit the transmembrane, tumor-associated carbonic anhydrase isoforms IX and XII over the cytosolic ones I and II. *Bioorg. Med. Chem. Lett.* **2010**, *20*, 4511−4514.

(32) Maresca, A.; Scozzafava, A.; Supuran, C. T. 7,8-Disubstituted- but not 6,7-disubstituted coumarins selectively inhibit the transmembrane, tumor-associated carbonic anhydrase isoforms IX and XII over the cytosolic ones I and II in the low nanomolar/subnanomolar range. *Bioorg. Med. Chem. Lett.* **2010**, *20*, 7255−7258.

(33) Touisni, N.; Maresca, A.; McDonald, P. C.; Lou, Y.; Scozzafava, A.; Dedhar, S.; Winum, J. Y.; Supuran, C. T. Glycosyl coumarin carbonic anhydrase IX and XII inhibitors strongly attenuate the growth of primary breast tumors. *J. Med. Chem.* **2011**, *54*, 8271−8277.

(34) Cottier, F.; Raymond, M.; Kurzai, O.; Bolstad, M.; Leewattanapasuk, W.; Jimenez-Lopez, C.; Lorenz, M. C.; Sanglard, D.; Vachova, L.; Pavelka, N.; Palkova, Z.; Mühlschlegel, F. A. The bZIP transcription factor Rca1p is a central regulator of a novel CO_2 sensing pathway in yeast. *PLOS Pathogens* **2012**, *8*, e10002485.

(35) Mogensen, E. G.; Janbon, G.; Chaloupka, J.; Steegborn, C.; Fu, M. S.; Moyrand, F.; Klengel, T.; Pearson, D. S.; Geeves, M. A.; Buck, J.; Levin, L. R.; Mühlschlegel, F. A. Fungal adenylyl cyclase integrates CO_2 sensing with cAMP signaling and virulence. *Curr. Biol.* **2005**, *15*, 2021−2026.
(36) Supuran, C. T. Bacterial carbonic anhydrases as drug targets: towards novel antibiotics? *Front. Pharmacol.* **2011**, *2*, 34.
(37) Hilvo, M.; Tolvanen, M.; Clark, A.; Shen, B.; Shah, G. N.; Waheed, A.; Sly, W. S.; Parkkila, S. Characterization of CA XV, a new GPI-anchored form of carbonic anhydrase. *Biochem. J.* **2005**, *392*, 83−92.
(38) Hilvo, M.; Salzano, A. M.; Innocenti, A.; Kulomaa, M. S.; Scozzafava, A.; Scaloni, A.; Parkkila, S.; Supuran, C. T. Cloning, characterization, post-translational modifications and inhibition studies of the latest mammalian carbonic anhydrase (CA) isoform, CA XV. *J. Med. Chem.* **2009**, *52*, 646−654.
(39) Scozzafava, A.; Menabuoni, L.; Mincione, F.; Briganti, F.; Mincione, G.; Supuran, C. T. Carbonic anhydrase inhibitors. Part 74. Synthesis of water-soluble, topically effective, intraocular pressure-lowering aromatic/heterocyclic sulfonamides containing cationic or anionic moieties: is the tail more important than the ring ? *J. Med. Chem.* **1999**, *42*, 2641−2650.
(40) Wilkinson, B. L.; Bornaghi, L. F.; Houston, T. A.; Innocente, A.; Supuran, C. T.; Poulsen, S.-A. A novel class of carbonic anhydrase inhibitors: Glycoconjugate benzene sulfonamides prepared by "click-tailing". *J. Med. Chem.* **2006**, *49*, 6539−6548.
(41) Wilkinson, B. L.; Bornaghi, L. F.; Houston, T. A.; Innocenti, A.; Vullo, D.; Supuran, C. T.; Poulsen, S.-A. Carbonic anhydrase inhibitors: inhibition of isozymes I, II, and IX with triazole-linked *O*-glycosides of benzene sulfonamides. *J. Med. Chem.* **2007**, *50*, 1651−1657.
(42) Wilkinson, B. L.; Bornaghi, L. F.; Houston, T. A.; Innocenti, A.; Vullo, D.; Supuran, C. T.; Poulsen, S.-A. Inhibition of membrane-associated carbonic anhydrase isozymes IX, XII and XIV with a library of glycoconjugate benzenesulfonamides. *Bioorg. Med. Chem. Lett.* **2007**, *17*, 987−992.
(43) Güzel, Ö.; Maresca, A.; Hall, R. A.; Scozzafava, A.; Mastrolorenzo, A.; Mühlschlegel, F. A.; Supuran, C. T. Carbonic anhydrase inhibitors. The *β*-carbonic anhydrases from the fungal pathogens *Cryptococcus neoformans* and *Candida albicans* are strongly inhibited by substituted-phenyl-1*H*-indole-5-sulfonamides. *Bioorg. Med. Chem. Lett.* **2010**, *20*, 2508−2511.
(44) Pacchiano, F.; Carta, F.; McDonald, P. C.; Lou, Y.; Vullo, D.; Scozzafava, A.; Dedhar, S.; Supuran, C. T. Ureido-substituted benzenesulfonamides potently inhibit carbonic anhydrase IX and show antimetastatic activity in a model of breast cancer metastasis. *J. Med. Chem.* **2011**, *54*, 1896−1902.
(45) Lou, Y.; McDonald, P. C.; Oloumi, A.; Chia, S. K.; Ostlund, C.; Ahmadi, A.; Kyle, A.; Auf dem Keller, U.; Leung, S.; Huntsman, D. G.; Clarke, B.; Sutherland, B. W.; Waterhouse, D.; Bally, M. B.; Roskelley, C. D.; Overall, C. M.; Minchinton, A.; Pacchiano, F.; Carta, F.; Scozzafava, A.; Touisni, N.; Winum, J. Y.; Supuran, C. T.; Dedhar, S. Targeting tumor hypoxia: suppression of breast tumor growth and metastasis by novel carbonic anhydrase IX inhibitors. *Cancer Res.* **2011**, *71*, 3364−3376.
(46) Weber, A.; Casini, A.; Heine, A.; Kuhn, D.; Supuran, C. T.; Scozzafava, A.; Klebe, G. Unexpected nanomolar inhibition of carbonic anhydrase by COX-2 selective Celecoxib: New pharmacological opportunities due to related binding site recognition. *J. Med. Chem.* **2004**, *47*, 550−557.
(47) Di Fiore, A.; Pedone, C.; D'Ambrosio, K.; Scozzafava, A.; De Simone, G.; Supuran, C. T. Carbonic anhydrase inhibitors: Valdecoxib binds to a different active site region of the human isoform II as compared to the structurally related, cyclooxygenase II "selective" inhibitor celecoxib. *Bioorg. Med. Chem. Lett.* **2006**, *16*, 437−442.
(48) Menchise, V.; De Simone, G.; Alterio, V.; Di Fiore, A.; Pedone, C.; Scozzafava, A.; Supuran, C. T. Carbonic anhydrase inhibitors: stacking with Phe131 determines active site binding region of inhibitors as exemplified by the X-ray crystal structure of a membrane-impermeant antitumor sulfonamide complexed with isozyme II. *J. Med. Chem.* **2005**, *48*, 5721−5727.
(49) Alterio, V.; Vitale, R. M.; Monti, S. M.; Pedone, C.; Scozzafava, A.; Cecchi, A.; De Simone, G.; Supuran, C. T. Carbonic anhydrase inhibitors: X-ray and molecular modeling study for the interaction of a fluorescent antitumor sulfonamide with isozyme II and IX. *J. Am. Chem. Soc.* **2006**, *128*, 8329−8335.
(50) Alterio, V.; De Simone, G.; Monti, S. M.; Scozzafava, A.; Supuran, C. T. Carbonic anhydrase inhibitors: inhibition of human, bacterial, and archaeal isozymes with benzene-1,3-disulfonamides—Solution and crystallographic studies. *Bioorg. Med. Chem. Lett.* **2007**, *17*, 4201−4207.
(51) Abbate, F.; Winum, J. Y.; Potter, B. V. L.; Casini, A.; Montero, J. L.; Scozzafava, A.; Supuran, C. T. Carbonic anhydrase inhibitors: X ray crystallographic structure of the adduct of human isozyme II with a EMATE, a dual inhibitor of carbonic anhydrases and steroid sulfatase. *Bioorg. Med. Chem. Lett.* **2004**, *14*, 231−234.
(52) Innocenti, A.; Hall, R. A.; Schlicker, C.; Scozzafava, A.; Steegborn, C.; Mühlschlegel, F. A.; Supuran, C. T. Carbonic anhydrase inhibitors. Inhibition and homology modeling studies of the fungal *β*-carbonic anhydrase from *Candida albicans* with sulfonamides. *Bioorg. Med. Chem.* **2009**, *17*, 4503−4509.
(53) Schlicker, C.; Hall, R. A.; Vullo, D.; Middelhaufe, S.; Gertz, M.; Supuran, C. T.; Muhlschlegel, F. A.; Steegborn, C. *J. Mol. Biol.* **2009**, *385*, 1207−1220.
(54) Pacchiano, F.; Aggarwal, M.; Avvaru, B. S.; Robbins, A. H.; Scozzafava, A.; McKenna, R.; Supuran, C. T. *Chem. Commun.* **2010**, *46*, 8371−8373.
(55) Carta, F.; Garaj, V.; Maresca, A.; Wagner, J.; Avvaru, B. S.; Robbins, A. H.; Scozzafava, A.; McKenna, R.; Supuran, C. T. Sulfonamides incorporating 1,3,5-triazine moieties selectively and potently inhibit carbonic anhydrase transmembrane isoforms IX, XII, and XIV over cytosolic isoforms I and II: solution and X-ray crystallographic studies. *Bioorg. Med. Chem.* **2011**, *19*, 3105−3119.
(56) Hen, N.; Bialer, M.; Yagen, B.; Maresca, A.; Aggarwal, M.; Robbins, A. H.; McKenna, R.; Scozzafava, A.; Supuran, C. T. Anticonvulsant 4-aminobenzenesulfonamide derivatives with branched-alkylamide moieties: X-ray crystallography and inhibition studies of human carbonic anhydrase isoforms I, II, VII, and XIV. *J. Med. Chem.* **2011**, *54*, 3977−3981.
(57) Supuran, C. T.; Casini, A.; Mastrolorenzo, A.; Scozzafava, A. COX-2 selective inhibitors, carbonic anhydrase inhibition and anticancer properties of sulfonamides belonging to this class of pharmacological agents. *Mini-Rev. Med. Chem.* **2004**, *4*, 625−632.
(58) Dogné, J. M.; Supuran, C. T.; Pratico, D. Adverse cardiovascular effects of the coxibs. *J. Med. Chem.* **2005**, *48*, 2251−2257.
(59) Dogne, J. M.; Hanson, J.; Supuran, C. T.; Pratico, D. Coxibs and cardiovascular side effects: From light to shadow. *Curr. Pharm. Des.* **2006**, *12*, 971−975.
(60) Knaus, E. E.; Innocenti, A.; Scozzafava, A.; Supuran, C. T. Phenylethynylbenzenesulfonamide regioisomers strongly and selectively inhibit the transmembrane, tumor-associated carbonic anhydrase isoforms IX and XII over the cytosolic isoforms I and II. *Bioorg. Med. Chem. Lett.* **2011**, *21*, 5892−5896.
(61) Dogne', J. M.; Thiry, A.; Pratico, D.; Masereel, B.; Supuran, C. T. Dual carbonic anhydrase-cyclooxygenase-2 inhibitors. *Curr. Top. Med. Chem.* **2007**, *7*, 885−891.
(62) Degani, I.; Fochi, R.; Spunta, G. Cationi eteroaromatici constanti di equilibrio catione-pseudobase *Boll. Sci. Fac. Chim. Ind. Bologna***1966**, *24*, 75; *Chem. Abstr.* **1967**, *66*, 46292.
(63) Fravolini, A.; Schiaffella, F.; Orzalesi, G.; Selleri, R.; Volpato, I. Oxime ether derivatives of thiochroman-4-ones as *β* -adrenergic blocking agents. *Eur. J. Med. Chem.* **1978**, *13* (4), 347−350.
(64) Da Settimo, A.; Marini, A. M.; Primofiore, G.; Da Settimo, F.; Salerno, S.; La Motta, C.; Pardi, G.; Ferrarini, P. L.; Mori, C. Synthesis of novel 5*H*,11*H*-Pyrido[2′,3′:2,3]thiopyrano[4,3-*b*]indoles by Fischer-indole cyclization. *J. Heterocycl. Chem.* **2000**, *37*, 379−382.
(65) Dalla Via, L.; Marini, A. M.; Salerno, S.; La Motta, C.; Condello, M.; Arancia, G.; Agostinelli, E.; Toninello, A. Synthesis and biological

activity of 1,4-dihydrobenzothiopyrano[4,3-*c*]pyrazole derivatives, novel pro-apoptotic mitochondrial targeted agents. *Bioorg. Med. Chem.* **2009**, *17*, 326−336.
(66) Primofiore, G.; Marini, A. M.; Da Settimo, F.; Salerno, S.; Bertini, D.; Dalla Via, L.; Marciani Magno, S. Synthesis of Novel 1,4-Dihydropyrido[3′,2′:5,6]thiopyrano[4,3-*c*]-pyrazoles and 5*H*-pyrido-[3′,2′:5,6]thiopyrano[4,3-*d*]pyrimidines as potential antiproliferative agents. *J. Heterocycl. Chem.* **2003**, *40*, 783−788.
(67) Da Settimo, A.; Marini, A. M.; Primofiore, G.; Da Settimo, F.; Salerno, S.; Simorini, F.; Pardi, G.; La Motta, C.; Bertini, D. Synthesis of novel pyrido[3′,2′:5,6]thiopyrano[3,2-*b*]indol-5(6*H*)-ones and 6*H*-pyrido[3′,2′:5,6]thiopyrano[4,3-*b*]quinolines, two new heterocyclic ring systems. *J. Heterocycl. Chem.* **2002**, *39*, 1001−1006.
(68) Primofiore, G.; Marini, A. M.; Salerno, S.; Da Settimo, F.; Bertini, D.; Dalla Via, L. Synthesis and antiproliferative evaluation of new aryl substituted pyrido[3′,2′:5,6]thiopyrano[4,3-*c*]pyrazoles. *J. Heterocycl. Chem.* **2005**, *42*, 1357−1361.
(69) Khalifah, R. J. The carbon dioxide hydration activity of carbonic anhydrase. I. Stop-flow kinetic studies on the native human isoenzymes B and C. *J. Biol. Chem.* **1971**, *246*, 2561−2573.
(70) Nishimori, I.; Minakuchi, T.; Vullo, D.; Scozzafava, A.; Innocenti, A.; Supuran, C. T. Carbonic anhydrase inhibitors. Cloning, characterization and inhibition studies of a new *β*-carbonic anhydrase from *Mycobacterium tuberculosis*. *J. Med. Chem.* **2009**, *52*, 3116−3120.
(71) Minakuchi, T.; Nishimori, I.; Vullo, D.; Scozzafava, A.; Supuran, C. T. Molecular cloning, characterization and inhibition studies of the Rv1284 *β*-carbonic anhydrase from *Mycobacterium tuberculosis* with sulfonamides and a sulfamate. *J. Med. Chem.* **2009**, *52*, 2226−2232.
(72) Carta, F.; Maresca, A.; Covarrubias, A. S.; Mowbray, S. L.; Jones, T. A.; Supuran, C. T. Carbonic anhydrase inhibitors. Characterization and inhibition studies of the most active *β*-carbonic anhydrase from *Mycobacterium tuberculosis*, Rv3588c. *Bioorg. Med. Chem. Lett.* **2009**, *19*, 6649−6654.
(73) Güzel, O.; Maresca, A.; Scozzafava, A.; Salman, A.; Balaban, A. T.; Supuran, C. T. Discovery of low nanomolar and subnanomolar inhibitors of the mycobacterial *β*-carbonic anhydrases Rv1284 and Rv3273. *J. Med. Chem.* **2009**, *52*, 4063−4067.
(74) Nishimori, I.; Minakuchi, T.; Onishi, S.; Vullo, D.; Cecchi, A.; Scozzafava, A.; Supuran, C. T. Carbonic anhydrase inhibitors. Cloning, characterization and inhibition studies of the cytosolic isozyme III with sulfonamides. *Bioorg. Med. Chem.* **2007**, *15*, 7229−7236.
(75) Supuran, C. T. Carbonic anhydrases: off-targets, add-on activities, or emerging novel targets? In *Polypharmacology in Drug Discovery*; Peters, J. U., Ed.; Wiley: Hoboken, NJ, 2012, pp 457−489.
(76) Avvaru, B. S.; Wagner, J. M.; Maresca, A.; Scozzafava, A.; Robbins, A. H.; Supuran, C. T.; McKenna, R. Carbonic anhydrase inhibitors. The X-ray crystal structure of human isoform II in adduct with an adamantyl analogue of acetazolamide resides in a new hydrophobic binding pocket. *Bioorg. Med. Chem. Lett.* **2010**, *20*, 4376−4381.
(77) Wagner, J.; Avvaru, B. S.; Robbins, A. H.; Scozzafava, A.; Supuran, C. T.; McKenna, R. Coumarinyl-substituted sulfonamides strongly inhibit several human carbonic anhydrase isoforms: solution and crystallographic investigations. *Bioorg. Med. Chem.* **2010**, *18*, 4873−4878.
(78) Köhler, K.; Hillebrecht, A.; Schulze Wischeler, J.; Innocenti, A.; Heine, A.; Supuran, C. T.; Klebe, G. Saccharin inhibits carbonic anhydrases: possible explanation for its unpleasant metallic aftertaste. *Angew. Chem., Int. Ed.* **2007**, *46*, 7697−7699.
(79) Eriksson, E.; Jones, T. A.; Liljas, A. Refined structure of human carbonic anhydrase II at 2.0 A resolution. *Proteins* **1988**, *4*, 274−282.
(80) Temperini, A.; Scozzafava, A.; Supuran, C. T. Carbonic anhydrase inhibitors. X-ray crystal studies of the carbonic anhydrase II—trithiocarbonate adduct—An inhibitor mimicking the sulfonamide and urea binding to the enzyme. *Bioorg. Med. Chem. Lett.* **2010**, *20*, 474−478.
(81) Emsley, P.; Cowtan, K. Coot: model-building tools for molecular graphics. *Acta Crystallogr., Sect. D: Biol. Crystallogr.* **2004**, *D60*, 2126−2132.
(82) Srivastava, D. K.; Jude, K. M.; Banerjee, A. L.; Haldar, M.; Manokaran, S.; Kooren, J.; Mallik, S.; Christianson, D. W. Structural analysis of charge discrimination in the binding of inhibitors to human carbonic anhydrases I and II. *J. Am. Chem. Soc.* **2007**, *129* (17), 5528−5537.
(83) Alterio, V.; Hilvo, M.; Di Fiore, A.; Supuran, C. T.; Pan, P.; Parkkila, S.; Scaloni, A.; Pastorek, J.; Pastorekova, S.; Pedone, C.; Scozzafava, A.; Monti, S. M.; De Simone, G. Crystal structure of the catalytic domain of the tumor-associated human carbonic anhydrase IX. *Proc. Natl. Acad. Sci. U.S.A.* **2009**, *106* (38), 16233−16238.
(84) Whittington, D. A.; Waheed, A.; Ulmasov, B.; Shah, G. N.; Grubb, J. H.; Sly, W. S.; Christianson, D. W. Crystal structure of the dimeric extracellular domain of human carbonic anhydrase XII, a bitopic membrane protein overexpressed in certain cancer tumor cells. *Proc. Natl. Acad. Sci. U.S.A.* **2001**, *98* (17), 9545−9550.
(85) Kulmacz, R. J.; Lands, W. E. Requirements for hydroperoxyde by the cyclooxygenase and peroxidase activities of prostaglandin H synthase. *Prostaglandins* **1983**, *25*, 531−549.
(86) McPherson, A. *Preparation and Analysis of Protein Crystals*, 1st Ed.; Wiley: New York, 1982.
(87) Otwinowski, Z.; Minor, W. Processing of X-ray diffraction data collected in oscillation mode. *Methods Enzymol.* **1997**, *276*, 307−326.
(88) Avvaru, B. S.; Kim, C. U.; Sippel, K. H.; Gruner, S. M.; Agbandje-McKenna, M.; Silverman, D. N.; McKenna, R. A short, strong hydrogen bond in the active site of human carbonic anhydrase II. *Biochemistry* **2010**, *49*, 249−251.
(89) Adams, P. D.; Afonine, P. V.; Bunkóczi, G.; Chen, V. B.; Davis, I. W.; Echols, N.; Headd, J. J.; Hung, L.-W.; Kapral, G. J.; Grosse-Kunstleve, R. W.; McCoy, A. J.; Moriarty, N. W.; Oeffner, R.; Read, R. J.; Richardson, D. C.; Richardson, J. S.; Terwilliger, T. C.; Zwart, P. H. PHENIX: A comprehensive Python-based system for macromolecular structure solution. *Acta Crystallogr., Sect. D: Biol. Crystallogr.* **2010**, *D66*, 213−221.
(90) Laskowski, R. A.; MacArthur, M. W.; Moss, D. S.; Thornton, J. M. PROCHECK: A program to check the stereochemical quality of protein structures. *J. Appl. Crystallogr.* **1993**, *26*, 283−291.